European Review for Medical and Pharmacological Sciences 2022; 26: 573-584

# Lnc-AC145676.2.1-6-3 can influence STX3-induced abnormal autophagy by sponging hsa-miR-1292-3p in intestinal aGVHD

X.-Q. SUN[1], G.-Q. TAN[2], Z. GAO[3], X.-J. LIU[4], M.-T. XIA[5], Y.-Y. ZHANG[1], R.-J. SUN[1], X. CUI[6]

[1]Department of Traditional Chinese Medicine, Shandong University of Traditional Chinese Medicine, Jinan, China
[2]Department of Spine Surgery, Affiliated Hospital of Shandong University of Traditional Chinese Medicine, Jinan, China
[3]Department of Neurosurgery, Affiliated Hospital of Shandong University of Traditional Chinese Medicine, Jinan, China
[4]Department of Cardiology, Affiliated Hospital of Shandong University of Traditional Chinese Medicine, Jinan, China
[5]The First Clinical Medical College, Shandong University of Traditional Chinese Medicine, Jinan, China
[6]Department of Hematology, Affiliated Hospital of Shandong University of Traditional Chinese Medicine, Jinan, China

**Abstract. – OBJECTIVE: Intestinal acute graft-versus-host disease (aGVHD) is a serious complication of allogeneic hematopoietic stem cell transplantation (allo-HSCT). Abnormal autophagy levels in intestinal aGVHD have been confirmed in many studies. LncRNAs exert coregulatory functions and participate in a variety of intracellular regulatory processes. In this study, we investigated how lnc-AC145676.2.1-6-3 regulates dysregulated STX3-related autophagy in aGVHD.**

**MATERIALS AND METHODS: First, we established a mouse model of aGVHD by transplanting a mononuclear cell suspension from Balb/c donor mice treated with 60Co X-rays into CB6F1 recipient mice. STX3-related indicators were analyzed by Western blotting (WB) and immunohistochemistry which confirmed that STX3 plays an important role in dysregulating autophagy in intestinal aGVHD. TNF-αinduced Caco-2 cells, which is an *in vitro* model of intestinal barrier dysfunction, were established to verify the effect of STX3. The direct interaction between the partners of lnc-AC145676.2.1-6-3-mediated hsa-miR-1292-3p and STX3 axis was evaluated by the Dual-Luciferase activity assay. We performed PCR, WB, and immunofluorescence in Caco-2 cells to determine whether the abnormal autophagy levels were influenced by lnc-AC145676.2.1-6-3.**

**RESULTS: The results showed that lnc-AC145676.2.1-6-3 could significantly suppress the number of autophagic vacuoles, the LC3-II/I ratio, and beclin1 levels by increasing STX3 levels.**

**CONCLUSIONS: Lnc-AC145676.2.1-6-3 may play an important role in intestinal aGVHD by targeting STX3.**

*Key Words:*
Intestinal acute graft-versus-host disease, STX3, Autophagy, Lnc-AC145676.2.1-6-3, Hsa-miR-1292-3p.

## Introduction

Intestinal acute graft-versus-host disease (aGVHD) is one of the most fatal complications in the early stage after allogeneic hematopoietic stem cell transplantation (allo-HSCT)[1]. The main manifestations are intractable diarrhea, severe colitis, hematochezia and intestinal obstruction, which can be life-threatening. Autophagy is the process by which a cell phagocytoses its own cytoplasmic proteins or organelles via encapsulation into vesicles, which fuse with lysosomes to form autophagic lysosomes that degrade the encapsulated contents. Our previous work suggests that autophagy protects the intestinal mucosa by degrading damaged organelles and other substances, which slows aGVHD progression[2]. Some studies[5,6] have shown that syntaxin 3 (STX3) affects autophagy[4] by regulating the PTEN-PI3K-AKT-mTOR signaling pathway. In addition, STX3 is associated with congenital diarrhea disorders[7] and intestinal epithelial differentiation diseases[8,9] and plays a role in the protection of the intestinal mucosa[10]. LncRNAs can act as miRNA sponges, whereby they regulate the target genes of miRNAs by binding the miRNAs

*Corresponding Author:* Xing Cui, MD; e-mail: cdz45@foxmail.com

and reducing their "silencing effect" on the target genes. These lncRNAs are also referred to as competitive endogenous RNAs (ceRNAs). Some studies have reported that the ceRNAs play an important role in hematological diseases[11]. In recent years, lncRNAs have been demonstrated to affect aGVHD. Therefore, we investigated whether lncRNAs can influence aGVHD pathology by regulating STX3-mediated autophagy.

## Materials and Methods

### Reagents and Antibodies

The lncRNA expression plasmid and negative control (NC) plasmid, the lncRNA wild type and lncRNA mutant Dual-Luciferase reporter plasmids, the STX3 wild type and STX3 mutant Dual-Luciferase reporter plasmids, the lncRNA-specific RT-PCR and quantitative RT-PCR (qRT-PCR) primers and the STX3 RT-PCR primers were obtained from Jierui Bioengineering Company, Limited (Shanghai, China). AKT1 rabbit monoclonal antibody (mAb) (A17909), phospho-AKT1-S473 rabbit mAb (AP0637), mTOR rabbit polyclonal antibody (pAb) (A11355), phospho-mTOR-S2448 rabbit pAb (AP0094), mouse anti-Bcl-2 antibody (bsm-33047M), STX3 pAb (15556-1-AP) and PTEN rabbit pAb (A2113) were purchased from Seville Biotechnology Company, Limited (Wuhan, Hubei, China). All-in-one miRNA qRT-PCR detection kits were purchased from GeneCopoeia (Rockville, MD, USA). MAbs against LC3-II, LC3-I, Beclin-1, P62, p-AMPK, AMPK, mTOR and GAPHD were purchased from Affinity Biosciences (Cincinnati, OH, USA). RIPA lysis buffer, avidin-biotinylated peroxidase, DAB, bovine serum albumin, polycarbonate lucifer yellow (dextran), the reverse transcription kit, the Millicell system and fluorescence plate reader were provided by Sparkjade (Jinan, Shandong, China). Rabbit anti-LC3B antibody was purchased from Abcam (Cambridge, UK). Alexa Fluor 488-conjugated AffiniPure goat anti-rabbit antibody and Cy3-conjugated goat anti-rabbit secondary antibody (BOSTER Biological, OH, USA) was used.

### Induction of the Mouse Model

The mice were purchased from Beijing Weitong Lihua Experimental Animal Technology Co., Ltd. (animal production license number was SCXK (Beijing) 2012-0001). Ten healthy Balb/c H-2d male mice were used as donors (weighing 18-22 g and aged 8-10 weeks), and 56 CB6F1 female mice were used as transplant recipients (weighing 18-22 g and aged 8-10 weeks); all mice were housed in SPF conditions. Inbred Balb/c H-2d mice were sacrificed by cervical dislocation, and bone marrow and spleen mononuclear cells were aseptically collected. Next, CB6F1 mice were irradiated once with $^{60}$Co X-rays, and then subjected to HSCT by infusing via tail vein the mononuclear cell suspension ($1\times10^7$ bone marrow cells + $1\times10^7$ spleen cells) obtained from donor Balb/c mice (above)[12]. The mice were randomly divided into a control group and a model group.

After the model was established, the clinical score for aGVHD was determined by observing weight loss, posture, activity, hair, skin integrity, and stool on the 15th day after transplantation using criteria established by Cooke et al[13]. Small intestinal tissues were collected from mice for histological analysis of the mucosa and scoring of pathological inflammation.

### Immunohistochemical Staining for STX3, PTEN, mTOR and LC3

Tissues of the small intestine (2-3 cm) were fixed with 70% ethanol overnight and then embedded in paraffin. The tissues were sliced into sections at a thickness of 4-6 μm before they were rinsed three times in PBS for 5 min and treated with 3% hydrogen peroxide in PBS for 15 min at 37°C to block endogenous peroxidase activity. The samples were then blocked with 5% bovine serum albumin and incubated with primary antibody in a humidified chamber at 4°C overnight. After several washes, the sections were incubated with secondary antibody for 60 min at 37°C, rehydrated in PBS and incubated with avidin-biotinylated peroxidase complex for 45 min at 37°C. After washing with PBS, peroxidase activity was evaluated by treating the sections with the chromogen DAB.

### Luciferase Reporter Constructs and Luciferase Activity Assay

The direct interactions between the constituents of the lnc-AC145676.2.1-6-3-mediated ceRNA network were evaluated by the Dual-Luciferase activity assay. A luciferase reporter vector (pmirGLO Dual-Luciferase miRNA Target Expression Vector; Promega) was used to generate the luciferase constructs. Lnc-AC145676.2.1-6-3 and the 3' UTR of STX3 were cloned by RT-PCR. Plasmids containing lnc-AC145676.2.1-6-3-WT, lnc-AC145676.2.1-6-3-mutant and the WT or mutant STX3-3' UTR were constructed. 293T cells were seeded onto 24-well plates and allowed to grow for ~24 h in antibiotic-free medium before

they were transfected. The constructed reporter vectors (300 ng) were cotransfected into cells with the miRNA (hsa-miR-1292-3p) mimics or NC mimics (100 nM) using Lipofectamine 2000 (2 μl). The cells were lysed ~24 h after transfection, and the luciferase activity was assayed using the Dual-Luciferase Reporter Assay System (Promega, Madison, WI, USA). Firefly luciferase activity was normalized to that of *Renilla* Luciferase. All experiments were performed independently in triplicate.

### Cell Lines and Culture

The human colon carcinoma cell line Caco-2 is used as an intestinal barrier dysfunction cell model when treated with TNF-α. Cells were grown in Dulbecco's modified Eagle's minimum essential medium (DMEM, pH 7.4) (Invitrogen, Carlsbad, CA, USA) supplemented with 25 mM glucose, 10% inactivated fetal bovine serum (FBS) (Lonza), 1% penicillin/streptomycin (PS) and 1% nonessential amino acid solution (Invitrogen, Carlsbad, CA, USA). After the cells were stimulated with TNF-α (100 ng/ml) for 21 h at 37°C, their viability was measured. Caco-2 cells were randomly divided into the following groups: control, model, lncRNA siRNA, siRNA-NC and lncRNA siRNA+miRNA inhibitor. The lncRNA siRNA+miRNA inhibitor group was treated with TNF-α after transfection.

### Cell Transfection

Caco-2 cells were assigned to the control (normal Caco-2 cells), model (Caco-2 cells stimulated with TNF-α (100 ng/ml) for 21 h at 37°C), siRNA (Caco-2 cells transfected with siRNA), siRNA-NC (Caco-2 cells transfected with NC siRNA), miR-1292-3p inhibitor (Caco-2 cells transfected with the miR-1292-3p inhibitor and then stimulated with TNF-α (100 ng/ml) for 21 h at 37°C), and miR-1292-3p inhibitor combined with siRNA (Caco-2 cells cotransfected with the miR-1292-3p inhibitor and siRNA) groups. The lnc-AC145676.2.1-6-3 mimic, lnc-AC145676.2.1-6-3 siRNA (si-lncRNA) and hsa-miR-1292-3p inhibitor were constructed by Gene Pharma (Shanghai, China).

### Cell Viability Assay

Caco-2 cells in the logarithmic growth phase were conventionally trypsinized, washed with PBS, pelleted by centrifugation, resuspended, and counted. Then, the cells were seeded into 96-well plates at $2\times10^3$ cells/well in a volume of 100 μl per well. After 24, 48, and 72 h of incubation, 10 μl of CCK-8 solution was added to each well and incubated for an additional 2 h after which the absorbance at a wavelength of 450 nm of each well was measured with a microplate reader and the mean was calculated for each group.

### Western Blotting (WB) Analysis

Intestinal tissue was homogenized in tissue protein extraction reagent (T-Per) solution supplemented with HALT protease inhibitors at 10 ml/g wet weight, Caco-2 cells were lysed using radio immunoprecipitation (RIPA) lysis buffer, and total protein was collected. Next, 20 μg of protein from each sample was loaded onto 10% sodium dodecyl sulphate-polyacrylamide gel electrophoresis (SDS-PAGE) gels, concentrated at 80 V for 20 min and separated at 120 V for ~1 h (as soon as the bromophenol blue color marker ran off the end of the gel). The samples were then transferred to polyvinylidene difluoride (PVDF) membranes at 110 V for 100 min at 4°C using the wet transfer method. Each membrane was blocked in 5% nonfat milk Tris Buffered Saline and Tween-20 (TBST) for 2 h prior to being incubated overnight at 4°C with primary antibodies against microtubule-associated protein 1 light chain 3 (LC3), P62, Beclin-1, STX3, PTEN, mTOR or AKT. Then, the membranes were washed 3 times with TBST for 10 min before they were incubated with diluted secondary antibodies in blocking solution for 2 h at room temperature. After the secondary antibody was fully washed away, a PTG ECL chemiluminescence detection kit was used to develop the blot, which was transferred to an imaging machine for exposure and analysis.

### Immunofluorescence Staining of LC3 in Cells

To identify autophagosome puncta in the cytoplasm, cells were fixed with polyformaldehyde for 15 min, permeabilized with 0.1% Triton X-100, washed three times with 0.5% Triton X-100 in PBS and finally stained with anti-LC3B antibody. Then, the cells were incubated with Alexa Fluor 488-conjugated AffiniPure goat anti-rabbit antibody in the dark for 2 h. Both the primary and secondary antibodies were diluted with 0.5% Triton X-100 in phosphate-buffered saline (PBS). After the glass slides were stained with DAPI and mounted with an anti-fluorescence sealant, images were captured directly by fluorescence microscopy.

### Transmission Electron Microscopy (TEM)

Autophagic vesicles were observed using TEM (Hitachi, HT7700). Treated cells were fixed with

2.5% glutaraldehyde and sodium pyruvate for 24 h, postfixed with 2% $OsO_4$ for 2 h, and then dehydrated. After the samples were washed and dried, TEM images were obtained.

### Statistical Analysis

The data are presented as the means ± standard deviation (SD) of three independent experiments. SPSS Statistics 26.0 software (IBM, Armonk, NY, USA) was used for the analyses. Student's *t*-test was used for comparisons between two groups.

## Results

### Detection of STX3-Related Autophagy In Vivo

The model group had more pronounced damage to the small intestinal mucosal epithelium structure with a higher level of inflammatory cell infiltration (Figure 1A). To examine autophagy *in vivo*, we collected small intestine tissues and blotted for autophagy-related proteins. The WB results showed that autophagy was decreased in the model group, as indicated by the decreased LC3II/I ratio, Beclin1 expression and PTEN expression induced by higher STX3 expression and the increased levels of mTOR and P62 ($p<0.01$) (Figure 1B). The immunohistochemistry results also showed that the protein levels of PTEN and LC3 were decreased and those of STX3 were increased in tissues of the model group compared with the control group. In addition, the mTOR pathway was activated ($p<0.01$) (Figure 1C). Additionally, there were more biphasic membrane autophagosomes with normal mitochondrial structure in the control group than in the model group (Figure 1D). Taken together, these results suggest that autophagy was inhibited in the model group.

### Construction and Verification of the LncRNA-miRNA-mRNA Interaction Network

LncRNAs most commonly interact with miRNAs to regulate downstream molecules. To further explore the mechanism of action of lnc-AC145676.2.1-6-3 in aGVHD, the target miRNAs and mRNAs of lnc-AC145676.2.1-6-3 were predicted by miRanda and TargetScan, which revealed 5 miRNAs: hsa-miR-1292-3p, hsa-miR-665, hsa-miR-4458, hsa-miR-3064-5p and hsa-miR-6504-5p. According to the cumulative weighted context++ score, we selected the top 1700 target genes of these miRNAs with TargetScan. KEGG analysis indicated that the most enriched term, "MAPK signaling pathway", was related to autophagy, and 19 target genes were identified as participating in this process. Cytoscape was used to visualize the ceRNA network of lnc-AC145676.2.1-6-3, hsa-miR-1292-3p and STX3 (Figure 2A). Among the identified downstream mRNAs, STX3 encodes a member of the STX family and is relevant to our research. TargetScan analysis predicted 3 target binding sites between STX3 and lnc-AC145676.2.1-6-3-interacting miRNAs (Table I). These results show that lnc-AC145676.2.1-6-3 might regulate the downstream hsa-miR-1292-3p/STX3 axis, which induces aGVHD. The binding sites of hsa-miR-1292-3p on STX3 were identified with the assistance of a bioinformatics prediction website. The results of the Dual-Luciferase reporter assay showed that hsa-miR-1292-3p mimics had no significant effect on the luciferase activity of the Mut-lnc-AC145676.2.1-6-3/STX3 plasmid group but led to a clear decrease in the luciferase activity of the WT-lnc-AC145676.2.1-6-3/STX3 plasmid group ($p < 0.01$) (Figure 2A). The changes in the luciferase activities of lncRNAs were the same as those mentioned above. All these data confirmed the existence of the lnc-AC145676.2.1-6-3/hsa-miR-1292-3p/STX3 axis.

### The Mechanism of Action of Lnc-AC145676.2.1-6-3/hsa-miR-1292-3p/STX3 In Vitro

After Caco-2 cells were induced by TNF-α, the downstream mechanism effects of the lnc-AC145676.2.1-6-3/hsa-miR-1292-3p/STX3 axis were assessed with transepithelial electrical resistance (TER), WB and immunofluorescence staining. Compared with the lncRNA siRNA + miRNA inhibitor and siRNA-NC groups, the lncRNA siRNA group had an increased TER ($p>0.05$).

To confirm the relationship of the lnc-AC145676.2.1-6-3/hsa-miR-1292-3p/STX3 axis, the levels of hsa-miR-1292-3p and STX3 were evaluated in Caco-2 cells. In the lncRNA siRNA group, miRNA expression was significantly increased compared with that in the model and siRNA-NC groups ($p<0.01$) (Figure 3B). Upon lncRNA interference, the level of miRNA binding to the lncRNA was significantly increased, while the level of STX3 was decreased (Figure 3C).

The levels of the autophagy-related proteins LC3II/I, Beclin1, P62, PTEN, Akt and mTOR as well as of STX3 were measured by WB. The results were similar to those observed *in vivo*, but in the lncRNA siRNA group, STX3 expression was

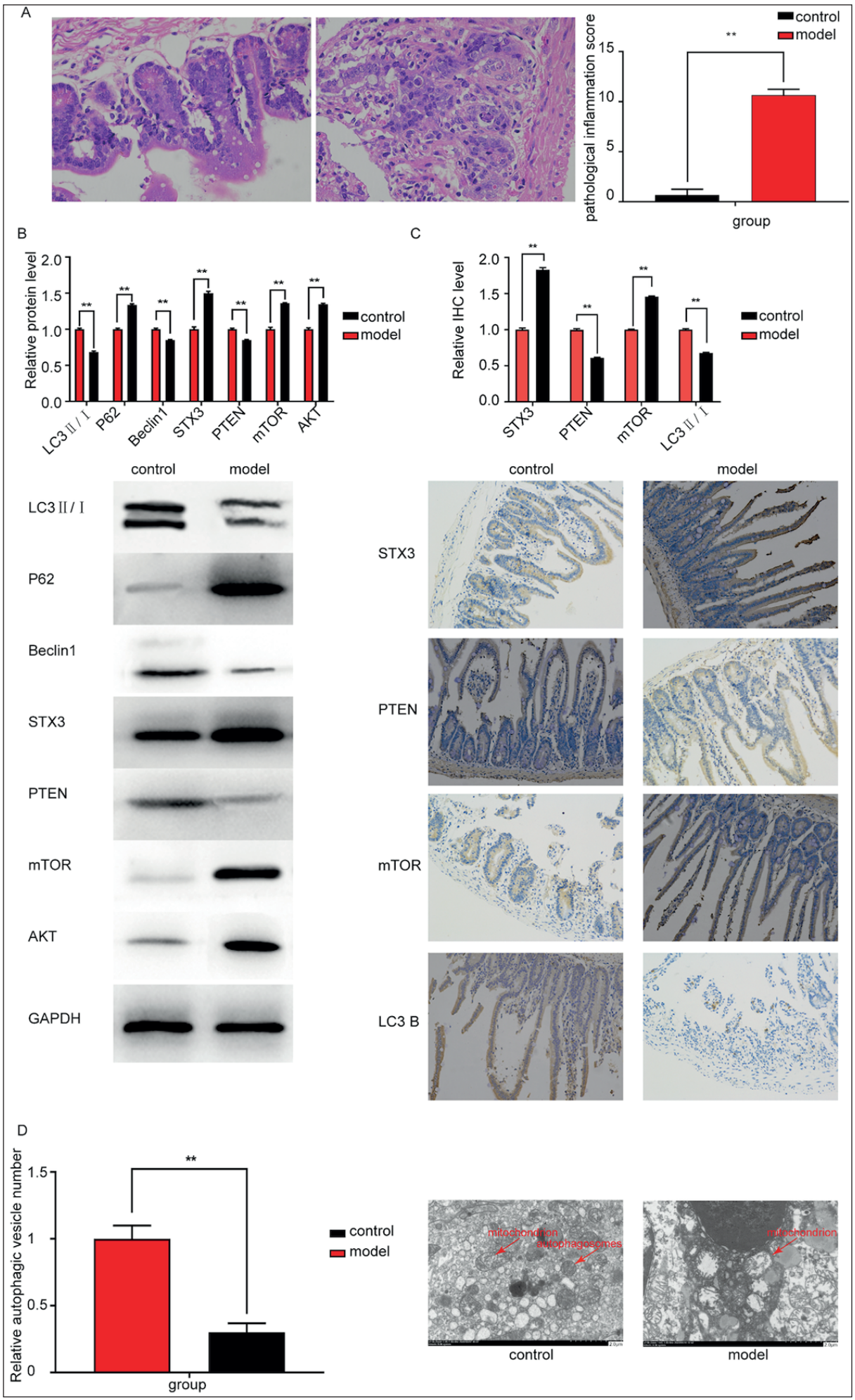


**Figure 1.** Detection of autophagy-related indexes in the small intestine of mice. **A,** Analysis of the mouse small intestine pathological score (magnification, 200×). **B,** Detection of the autophagy-related proteins LC3II/I, Beclin1, AKT, PTEN, mTOR and STX3 by Western blotting. **C,** Immunohistochemical analysis (magnification, 200×). **D,** Detection of autophagic vesicles. (**$p$<0.01, *$p$<0.05).

**Table I.** The binding sites between STX3 and hsa-miR-665, hsa-miR-4458 and hsa-miR-3064-5p as predicted by TargetScan.

| | Predicted consequential pairing of target region (top) and miRNA (bottom) | Site type | Context++ score | Context++ score percentile | Weighted context++score | Conserved branch length | Pct |
|---|---|---|---|---|---|---|---|
| Position 257-264 of STX3 3' UTR hsa-miR-665 | 5' ...UCUCAAGUACCUUUU-CUCCUGGA…<br>\|\|\| \|\|\|\|\|\|\|<br>3' UCCCCGGAGUCGGAGGACCA | 8mer | -0.33 | 98.00 | -0.33 | 3.18 | N/A |
| Position 366-373 of STX3 3' UTR hsa-miR-4458 | 5' ...AGGUGCUGUAUUUUUCUACCUCA...<br>\|\|\|\|\|\|\|<br>3' UUCUUUGAUGAUGGAGU | 8mer | -0.54 | 99.00 | -0.54 | 5.74 | 0.95 |
| Position 2253-2259 of STX3 3' UTR hsa-miR-3064-5p | 5' ...AUUCUGGGUCCUAGAAGCCAGAU...<br>\|\|\|\|\|\|<br>3' AACGUGUGGUGUUGUCGGUCU | 7mer-A1 | -0.03 | 51.00 | 0.00 | 4.98 | 0.18 |

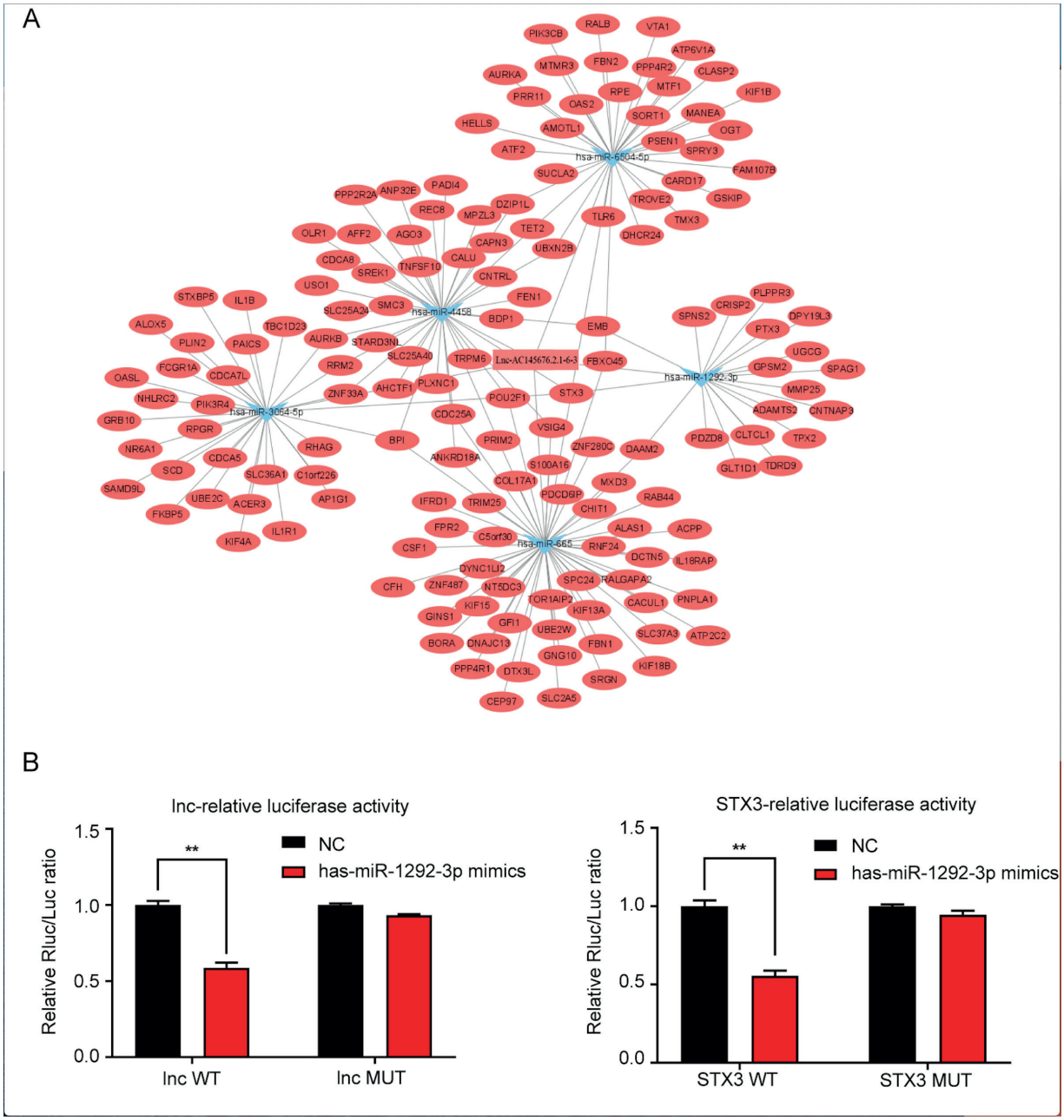


**Figure 2.** CeRNA mechanism and Dual-Luciferase assays. **A,** The lncRNA-miRNA-mRNA network predicted by miRanda and TargetScan is presented as a map constructed with Cytoscape software. **B,** Relative Luciferase activity of the lncRNA and STX3 reporters (**$p$<0.01, *$p$<0.05).

significantly decreased, whereas the expression of autophagy-related proteins was significantly increased, indicating that when inhibition of lnc-AC145676.2.1-6-3 increased the level of autophagy ($p$<0.01) (Figure 3D).

### *Autophagy Level Test in Caco-2 Cells*

In the lncRNA siRNA group, the relative number of LC3 puncta per cell was significantly increased compared with that in the model, siRNA-NC, and lncRNA siRNA +mRNA inhibitor groups, as observed by immunofluorescence microscopy (Figure 4A). To examine autophagy *in vitro*, we used Caco-2 cells and detected autophagy by TEM. There were more biphasic membrane autophagosomes with normal mitochondrial structure in the lncRNA siRNA group than in the siRNA-NC and lncRNA siRNA + mRNA inhib-

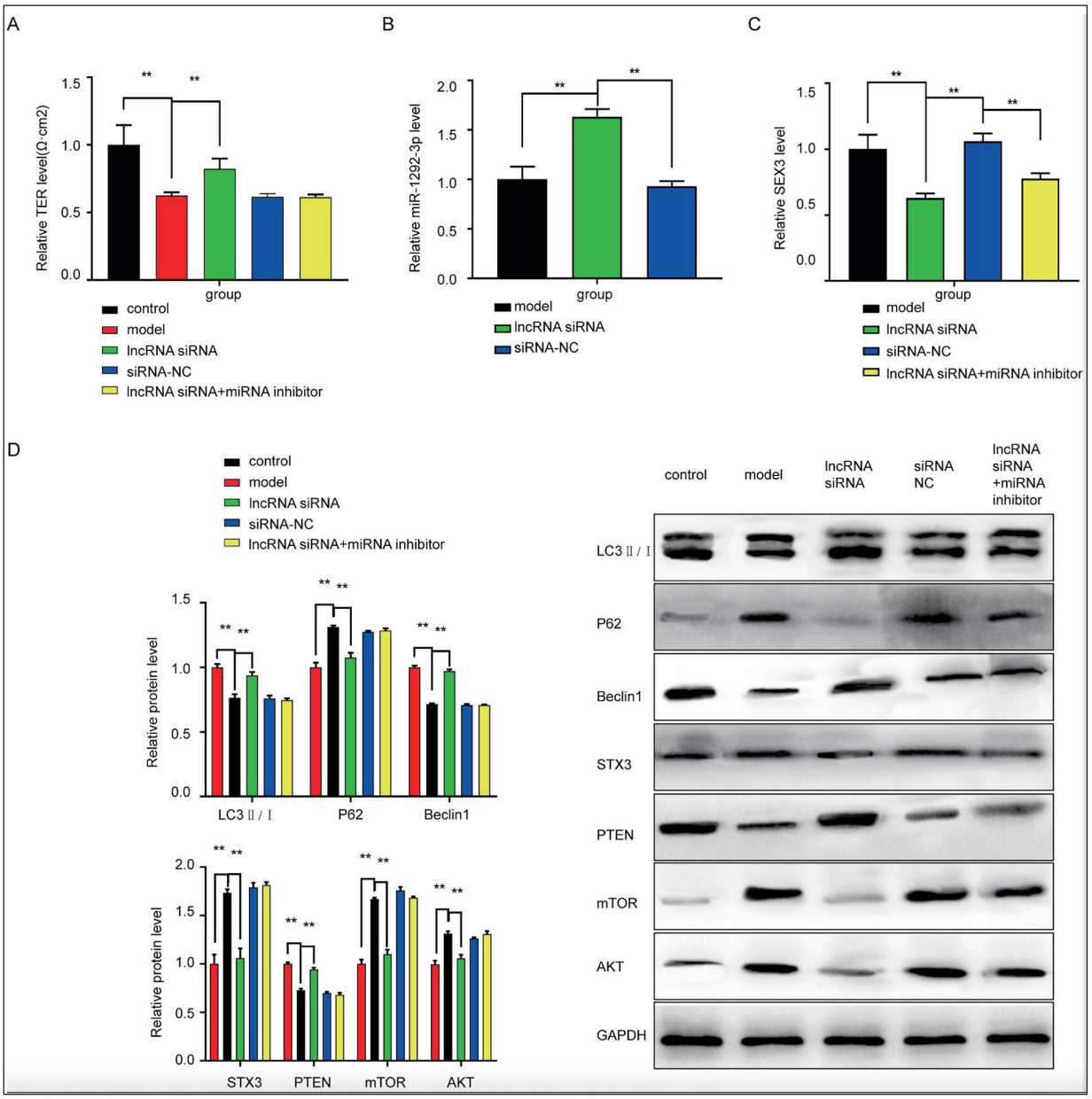


**Figure 3.** Detection of autophagic protein levels in Caco-2 cells. **A,** TER test in Caco-2 cells. **B,** The level of miRNA after lncRNA was knocked down. **C,** The level of STX3 after lncRNA was knocked down. **D,** Detection of the autophagy-related proteins LC3II/I, Beclin1, AKT, PTEN, mTOR and STX3 by Western blotting (**$p$<0.01, *$p$<0.05).

itor groups ($p$<0.01) (Figure 4B). These results confirm that when lnc-AC145676.2.1-6-3 was silenced, the level of STX3 was decreased leading to increased levels of autophagy and consequent inhibition of aGVHD progression.

## Discussion

aGVHD is the primary complication of allo-HSCT and the main cause of death after HSCT. aGVHD mainly manifests in the gastrointestinal tract, skin, and liver. There have been many studies on its pathogenesis, which may be affected by the intestinal flora, inflammatory reactions and so on[14,15]. The most common type of aGVHD is intestinal aGVHD[16], the symptoms of which are refractory diarrhea, severe colitis, hematochezia and intestinal obstruction that will affect the implantation and endanger the life of the patient[17].

STX3 has been shown to be involved in autophagy and can regulate the PTEN-PI3K-AKT-mTOR

signaling pathway[4]. Several studies[5,6] have reported that the PTEN-PI3K-AKT-mTOR pathway and many members of the STX family are closely related to autophagy. For example, STX2 affects autophagy through the NF-κB pathway[18], STX17 has been associated with autophagy signaling[19], and STX6 has been shown to promote autophagy[20]. Furthermore, STX3 is associated with congenital diarrhea[7], intestinal epithelial differentiation diseases[8,9], and intestinal microvilli inclusion body diseases[21] and participates in the protection of intestinal mucosa[10]. Inhibition of PTEN can enhance Akt phosphorylation and accelerate GVHD progression[22], and excessive activation of Akt/mTOR signaling may be related to the occurrence of aGVHD[23]. In a mouse model of aGVHD (Figure 1A), the level of PTEN was decreased, the levels of Akt and STX3 were increased, and the mTOR pathway was activated (Figure 1B,C). A TNF-α-induced Caco-2 *in vitro* cell model was used to mimic the damage in the intestinal mucosal barrier and elicited similar results as those of the *in vivo* experiments (Figure 3D).

Autophagy, as an intracellular degradation pathway necessary for cellular homeostasis, can reduce inflammasome activation by removing inflammasome components or cytokines associated with intracellular pathogenic molecules. A previous study found that after ectopic expression of inhibitors of apoptosis proteins (IAPs), the level of LC3 (an autophagic gene and marker of disease) was decreased, which suggests that aGVHD

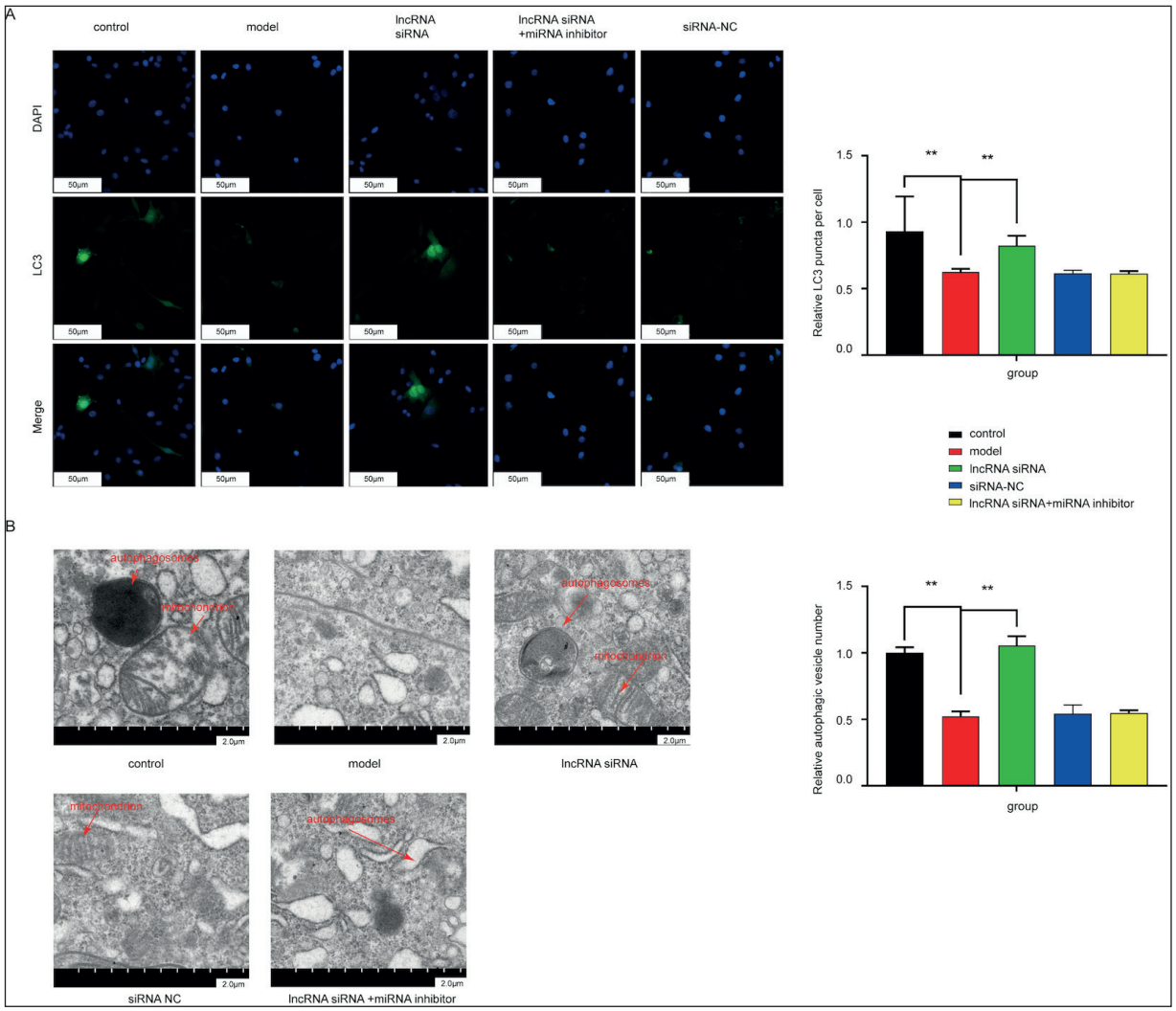


**Figure 4.** Detection of autophagic vesicles and immunofluorescence staining of Caco-2 cells. **A,** Immunofluorescence staining of LC3 (magnification, 200×). **B,** Detection of autophagic vesicles by TEM and the number of autophagic vesicles (magnification, 7000×). (**$p$<0.01, *$p$<0.05).

not only activates apoptosis but also is accompanied by the inhibition of autophagy[24], which was also observed in our results (Figure 4A). Some studies have suggested that autophagy activation attenuates intestinal mucosal barrier dysfunction by preventing and reducing oxidative stress[25,26]. At the same time, inflammasome activation can upregulate autophagy to reduce the damage to host tissues caused by an exacerbated inflammatory response[27]. Our experiments showed that the expression levels of the autophagy-related factors LC3, p62, and Beclin1 were changed and that mTOR was activated in aGVHD (Figure 1B, C and Figure 3D). Combined with the TEM and immunohistochemistry results, these findings indicate that the autophagy level was changed. Therefore, the decrease in mitochondrial autophagy may be involved in the pathogenesis of intestinal aGVHD, and the specific mechanism may be abnormal mitochondrial autophagy, which results in a decreased ability to scavenge damaged mitochondria and to inhibit oxidative damage and inflammatory damage to the intestinal mucosal barrier in aGVHD, resulting in the occurrence and aggravation of intestinal rejection. We found that the mitochondria in cells subjected to aGVHD were seriously damaged, which may be one of drivers of the occurrence of aGVHD (Figure 1D and Figure 4B).

Previous studies have shown that lncRNAs play an important role in the occurrence and development of aGVHD[28], but research on the specific mechanism involved is still rare and with little to no evidence on the role of lncRNAs with respect to STX3 mRNA in aGVHD. An increased level of lnc-AC145676.2.1-6-3 was observed in aGVHD in our previous study. We used miRanda and TargetScan to predict the target miRNAs and mRNAs of lnc-AC145676.2.1-6-3; the top miRNA was hsa-miR-1292-3p. Among the downstream mRNAs, STX3 was relevant to our research. These results suggested that lnc-AC145676.2.1-6-3 might regulate the downstream hsa-miR-1292-3p/STX3 axis (Figure 2A). After the relationship of lnc-AC145676.2.1-6-3/hsa-miR-1292-3p/STX3 was verified by a luciferase reporter assay (Figure2B), the *in vivo* data confirmed that lnc-AC145676.2.1-6-3 can influence STX3 function by sponging hsa-miR-1292-3p. The lncRNA siRNA group data showed that when the level of autophagy was increased and the level of STX3 was decreased, the aGVHD progression was ameliorated (Figure 3 and Figure 4).

We conducted a preliminary experimental study on the mechanism by which lnc-ac145676.2.1-6-3 affects the process of intestinal aGVHD, which provides a new approach for the clinical treatment of intestinal GVHD. However, the studies on successfully treating this disease lack sufficient data regarding its molecular targets, and detailed experiments on how to utilize this lncRNA and its target genes to treat aGVHD *in vivo*, will be part of our future directions.

## Conclusions

STX3-induced increases in autophagy levels via the PTEN/AKT/mTOR pathway in aGVHD were confirmed in animal models and Caco-2 cells. Then, from our previous study, upregulated lnc-AC145676.2.1-6-3 was verified to regulate the hsa-miR-1292-3p/STX3 axis by bioinformatic analysis and luciferase reporters. After conducting tests *in vivo*, we concluded that lnc-AC145676.2.1-6-3 plays an important role in STX3-induced increases in autophagy levels in aGVHD.

### Funding

The work was supported by the National Natural Science Foundation of China (No.81774080), the Taishan Scholar Program (tsqn201812145), the Study Abroad Funding by the People's Government of Shandong Province, and the Shandong Province Key Research and Development Program (No. 2019GSF108162).

### Conflicts of Interest

The authors declare no conflicts of interest.

### Availability of Data and Material

We would like support with depositing and managing their data of individual users as well as submit datasets to the Editorial Manager. All data are available from the corresponding author upon reasonable request.

### Authors' Contributions

Dr. Xing Cui designed and performed the experiments, analyzed the data, and wrote the manuscript; Master Xiaoqi Sun wrote the manuscript; Dr. Guoqing Tan provided the experimental site and some equipment; Dr. Zong Gao obtained and tested mouse tissue samples; Dr. Xiujuan Liu, Master Yanyu Zhang, RunjieSun and Mengting Xia provided vital new reagents and performed experiments. All authors have read and approved the manuscript and ensure the accuracy of the information presented.

### Ethics Approval

This study was approved by the Ethics Committee of the Affiliated Hospital of Shandong University of Traditional Chinese Medicine (Ethics number: awe-2019-037).

### Consent to Participate

All authors agree to publish in your journal.

## References


1) Liu A, Meyer E, Johnston L, Brown J, Gerson LB. Prevalence of graft versus host disease and cytomegalovirus infection in patients post-haematopoietic cell transplantation presenting with gastrointestinal symptoms. Aliment Pharmacol Ther 2013; 38: 955-966.
2) Lin Y, Wang B, Shan W, Tan Y, Feng J, Xu L, Wang L, Han B, Zhang M, Yu J, Yu X, Huang H. mTOR inhibitor rapamycin induce polymorphonuclear myeloid-derived suppressor cells mobilization and function in protecting against acute graft-versus-host disease after bone marrow transplantation. Clin Immunol 2018; 187: 122-131.
3) Nan H, Han L, Ma J, Yang C, Su R, He J. STX3 represses the stability of the tumor suppressor PTEN to activate the PI3K-Akt-mTOR signaling and promotes the growth of breast cancer cells. Biochim Biophys Acta Mol Basis Dis 2018; 1864: 1684-1692.
4) Wang L, Tang B, Han H, Mao D, Chen J, Zeng Y, Xiong M. miR-155 Affects Osteosarcoma MG-63 Cell Autophagy Induced by Adriamycin Through Regulating PTEN-PI3K/AKT/mTOR Signaling Pathway. Cancer Biother Radiopharm 2018; 33: 32-38.
5) Song BQ, Chi Y, Li X, Du WJ, Han ZB, Tian JJ, Li JJ, Chen F, Wu HH, Han LX, Lu SH, Zheng YZ, Han ZC. Inhibition of Notch Signaling Promotes the Adipogenic Differentiation of Mesenchymal Stem Cells Through Autophagy Activation and PTEN-PI3K/AKT/mTOR Pathway. Cell Physiol Biochem 2015; 36: 1991-2002.
6) Dhekne HS, Pylypenko O, Overeem AW, Zibouche M, Ferreira RJ, van der Velde KJ, Rings E, Posovszky C, van der Sluijs P, Swertz MA, Houdusse A, van IJzendoorn S. MYO5B, STX3, and STXBP2 mutations reveal a common disease mechanism that unifies a subset of congenital diarrheal disorders: A mutation update. Hum Mutat 2018; 39: 333-344.
7) Wiegerinck CL, Janecke AR, Schneeberger K, Vogel GF, van Haaften-Visser DY, Escher JC, Adam R, Thoni CE, Pfaller K, Jordan AJ, Weis CA, Nijman IJ, Monroe GR, van Hasselt PM, Cutz E, Klumperman J, Clevers H, Nieuwenhuis EE, Houwen RH, van Haaften G, Hess MW, Huber LA, Stapelbroek JM, Muller T, Middendorp S. Loss of syntaxin 3 causes variant microvillus inclusion disease. Gastroenterology 2014; 147: 65-68.
8) Mosa MH, Nicolle O, Maschalidi S, Sepulveda FE, Bidaud-Meynard A, Menche C, Michels BE, Michaux G, de Saint BG, Farin HF. Dynamic Formation of Microvillus Inclusions During Enterocyte Differentiation in Munc18-2-Deficient Intestinal Organoids. Cell Mol Gastroenterol Hepatol 2018; 6: 477-493.
9) Nazir S, Kumar A, Chatterjee I, Anbazhagan AN, Gujral T, Priyamvada S, Saksena S, Alrefai WA, Dudeja PK, Gill RK. Mechanisms of Intestinal Serotonin Transporter (SERT) Upregulation by TGF-beta1 Induced Non-Smad Pathways. PLoS One 2015; 10: e0120447.
10) Zhou S, Fang J, Sun Y, Li H. Integrated Analysis of a Risk Score System Predicting Prognosis and a ceRNA Network for Differentially Expressed lncRNAs in Multiple Myeloma. Front Genet 2020; 11: 934.
11) Le Texier L, Lineburg KE, MacDonald KP. Harnessing bone marrow resident regulatory T cells to improve allogeneic stem cell transplant outcomes. Int J Hematol 2017; 105: 153-161.
12) Dertschnig S, Nusspaumer G, Ivanek R, Hauri-Hohl MM, Hollander GA, Krenger W. Epithelial cytoprotection sustains ectopic expression of tissue-restricted antigens in the thymus during murine acute GVHD. Blood 2013; 122: 837-841.
13) Cooke KR, Kobzik L, Martin TR, Brewer J, Delmonte JJ, Crawford JM, Ferrara JL. An experimental model of idiopathic pneumonia syndrome after bone marrow transplantation: I. The roles of minor H antigens and endotoxin. Blood 1996; 88: 3230-3239.
14) Nomura S, Ishii K, Fujita S, Nakaya A, Satake A, Ito T. Associations between acute GVHD-related biomarkers and endothelial cell activation after allogeneic hematopoietic stem cell transplantation. Transpl Immunol 2017; 43-44: 27-32.
15) Gooptu M, Koreth J. Translational and clinical advances in acute graft-versus-host disease. Haematologica 2020; 105: 2550-2560.
16) Liu A, Meyer E, Johnston L, Brown J, Gerson LB. Prevalence of graft versus host disease and cytomegalovirus infection in patients post-haematopoietic cell transplantation presenting with gastrointestinal symptoms. Aliment Pharmacol Ther 2013; 38: 955-966.
17) Sun X, Su Y, Liu X, Zhang Y, He Y, Han W, Chen Q, Chen H, Wang Y, Cheng Y, Liu F, Wang F, Chen Y, Zhang G, Mo X, Fu H, Chen Y, Wang J, Zhu X, Xu L, Liu K, Huang X, Zhang X. Overt gastrointestinal bleeding following haploidentical haematopoietic stem cell transplantation: incidence, outcomes and predictive models. Bone Marrow Transplant 2021; 56: 1341-1351.
18) Wang Y, Xu H, Jiao H, Wang S, Xiao Z, Zhao Y, Bi J, Wei W, Liu S, Qiu J, Li T, Liang L, Ye Y, Liao W, Ding Y. STX2 promotes colorectal cancer metastasis through a positive feedback loop that activates the NF-kappaB pathway. Cell Death Dis 2018; 9: 664.
19) Arasaki K, Tagaya M. Legionella blocks autophagy by cleaving STX17 (syntaxin 17). Autophagy 2017; 13: 2008-2009.
20) Nozawa T, Minowa-Nozawa A, Aikawa C, Nakagawa I. The STX6-VTI1B-VAMP3 complex facilitates

xenophagy by regulating the fusion between recycling endosomes and autophagosomes. Autophagy 2017; 13: 57-69.
21) Michaux G, Massey-Harroche D, Nicolle O, Rabant M, Brousse N, Goulet O, Le Bivic A, Ruemmele FM. The localisation of the apical Par/Cdc42 polarity module is specifically affected in microvillus inclusion disease. Biol Cell 2016; 108: 19-28.
22) Zhu H, Lan L, Zhang Y, Chen Q, Zeng Y, Luo X, Ren J, Chen S, Xiao M, Lin K, Chen M, Li Q, Chen Y, Xu J, Zheng Z, Chen Z, Xie Y, Hu J, Yang T. Epidermal growth factor stimulates exosomal microRNA-21 derived from mesenchymal stem cells to ameliorate aGVHD by modulating regulatory T cells. FASEB J 2020; 34: 7372-7386.
23) Xu YJ, Chen FP, Chen Y, Fu B, Liu EY, Zou L, Liu LX. A Possible Reason to Induce Acute Graft-vs.-Host Disease After Hematopoietic Stem Cell Transplantation: Lack of Sirtuin-1 in CD4(+) T Cells. Front Immunol 2018; 9: 3078.
24) Toubai T, Rossi C, Oravecz-Wilson K, Liu C, Zajac C, Wu SJ, Sun Y, Fujiwara H, Tamaki H, Peltier D, Riwes M, Henig I, Brabbs S, Duckett CS, Wang S, Reddy P. IAPs protect host target tissues from graft-versus-host disease in mice. Blood Adv 2017; 1: 1517-1532.
25) Huang L, Jiang Y, Sun Z, Gao Z, Wang J, Zhang D. Autophagy Strengthens Intestinal Mucosal Barrier by Attenuating Oxidative Stress in Severe Acute Pancreatitis. Dig Dis Sci 2018; 63: 910-919.
26) Tang B, Li Q, Zhao XH, Wang HG, Li N, Fang Y, Wang K, Jia YP, Zhu P, Gu J, Li JX, Jiao YJ, Tong WD, Wang M, Zou QM, Zhu FC, Mao XH. Shiga toxins induce autophagic cell death in intestinal epithelial cells via the endoplasmic reticulum stress pathway. Autophagy 2015; 11: 344-354.
27) She H, He Y, Zhao Y, Mao Z. Release the autophage brake on inflammation: The MAPK14/p38alpha-ULK1 pedal. Autophagy 2018; 14: 1097-1098.
28) Li J, Seligson N, Zhang X, Johnson J, Vangundy Z, Wang D, Phelps M, Hofmeister C, Sadee W, Poi MJ. Association of ANRIL Polymorphism With Overall Survival in Adult Patients With Hematologic Malignancies After Allogeneic Hematopoietic Stem Cell Transplantation. Anticancer Res 2020; 40: 5707-5713.